

INFLUENCE OF STEEL FIBRES ON SELF-COMPACTING CONCRETE BEAMS WITH LONGITUDINAL REINFORCEMENT FAILING IN SHEAR

*Venkata Siva Kumar Anumolu , Ulvis Skadiņš 

Latvia University of Life Sciences and Technologies, Latvia

*Corresponding author's email: Sivakumaranumolu95@gmail.com

Abstract

Fibre-reinforced concrete, if properly designed, can be a very efficient construction material. However, there are challenges to using them in load-bearing structures due to the high dispersion of strength properties. Therefore, structural design methods need to be calibrated with experimental data. This research aims to investigate factors that influence the shear capacity of steel fibre-reinforced concrete (SFRC) beams with conventional longitudinal reinforcement (Hybrid reinforcement). An experimental test program of 30 large beam specimens, 96 prism specimens, 45 cores, and 15 cubes was conducted. Beams were tested in a three-point bending configuration resulting in a shear failure. Additionally, the crack propagation and crack width were examined. Two types of fibres were used with diameter of 0.5 mm and length of 50 mm and 35 mm. The fibres at volume fractions of 40 kg m⁻³ and 80 kg m⁻³ were tested and compared with the specimens that were without steel fibres. Tools like a digital image correlation (DIC) were employed to monitor the crack propagation, and a web plot designer was utilized to analyse the fibre count. The results demonstrate that the fibres contributed up to 120% for the increase of shear capacity with fibre dosage of 40 kg/m³, and up to 220% when the dosage was 80 kg m⁻³. Beams with long fibres (50 mm) showed more abrupt failure caused by rupture of fibres. The results of the current study reveal that there are phenomena that cannot be captured based on the standard prism tests. These results are going to be used to calibrate numerical models in nonlinear models in non-linear finite element analysis software in future studies.

Keywords: experimental tests, hybrid reinforcement, self-compacting concrete, shear capacity, steel fibre reinforced concrete.

Introduction

Concrete by nature is a very brittle material due to its low tensile strength. That is true also for concrete structures subjected to shear stresses because, in most cases, the shear capacity is governed by tensile strength. However, tensile and shear stresses can be resisted by several forms of reinforcement. Compared to conventional steel-reinforcement, fibres of various materials can be utilized as the primary reinforcement or as a supplement. For structural purposes, steel fibre reinforced concrete (SFRC) is the most commonly used. Besides other advantages, steel fibres enhance shear strength and moderate crack formation; they can resist brittle failure (Cohen & Aoude, 2012).

It is well established that SFRC is efficient to increase shear capacity of beams (Baston et al., 1972; Swamy & Bahia, 1985; Narayanan & Darwish, 1987; Kwak et al., 2002; Sahoo & Sharma, 2014). However, there is still a challenge to predict the capacity and post-peak behaviour of reinforced SFRC beams subjected to shear. The shear phenomena is complicated and challenging even in conventional reinforced concrete beams due to the many affecting parameters like concrete strength, shear span to depth ratio, amount of longitudinal reinforcement, aggregate size, size of the cross-section, and others. With the use of SFRC, several other parameters are introduced, which increase the complexity of the prediction.

There are several methods to estimate the effect of the SFRC beams subjected to shear given in standards and technical literature (European Committee for Standardization, 2023; Fédération internationale du béton, 2013). Many approaches and models are being proposed by researchers to predict the shear behaviour (Kwak et al., 2002; Sahoo & Sharma, 2014; Shahnewaz & Alam, 2014; Minelli & Plizzari, 2010). Slater et al. (2012) used linear and non-linear

regression analysis on the previous experimental data to develop a shear strength prediction model for beams. Kim et al. (2012) used the smeared crack model and truss model and developed a shear behaviour model for SFRC beams by applying material constitutive equations and by modifying conditions for strain compatibility and force equilibrium. Finite element method (FEM) is being widely utilized by numerous researchers because it allows for nonlinear material properties to be defined, which is important in case of SFRC (Zhang et al., 2020; Skadins & Cervenka, 2024). Two main groups of FEM nonlinear analysis software can be distinguished based on the methods of analysis: smeared crack method (Rashid, 1968; Cervenka & Gerstle, 1971) and discrete crack method (Saouma, 1981; Lee et al., 2016).

However, the problem to predict the shear behaviour of SFRC beams is well illustrated in the results of the blind competition organised by fib TG 2.4.1 – Modelling of Fibre Reinforced Concrete Structures. Almost all of the participants overestimated the load bearing capacity and the stiffness of the beams tested in the competition significantly (Barros et al., 2020). Many analyses predicted that the failure will be caused by bending moment suggesting that the shear capacity was even higher. The problem may not be in the nonlinear analysis software but in the input parameters that are defined for SFRC.

The aim of the study is to use a series of experimental tests of SFRC beams reinforced with conventional longitudinal rebars without shear links subjected to shear failure and evaluate the parameters affecting shear capacity. The results of this study are going to be used to evaluate the predictions given by nonlinear analysis using finite element method in future studies.

Materials and Methods

The influence of fibres on the shear capacity of beams is evaluated by conducting an experimental test program. There were ten series of 2.0 m long beams manufactured to be tested in three-point bending. The series were designed to evaluate the influence of shear span to depth ratio, fibre content and the length of fibres.

Specimens

The shape of the beams was designed with two heights, where the part with the bigger height was reinforced with shear links, while the other part with smaller height had no shear reinforcement except for the steel fibres. It was expected that the shear failure occurs in this part. The geometry and the reinforcement layout are given in Figure 1.

The heights of the beams (shear side/other side) were 300/500 mm and 400/600 mm, and the width of the beams was 150 mm. The beams were made of five types of materials, which are described below. Altogether there were 30 beam specimens grouped in ten series with three specimens in each series. The description of the beam series is given in Table 1.

The specimens were reinforced with longitudinal rebars on top (2Ø20 mm) and bottom (4Ø20 mm) to prevent them from failing due to bending moment. The

top reinforcement was tied with horizontal links to minimize the risk of buckling due compressive stresses. The shear links (Ø10, @100 mm) were provided only on one part of the span to prevent it from failure and diagonal cracking. Nominal concrete cover of the longitudinal reinforcement was 30 mm.

Figure 1

Beams specimens used in experimental programme with dimensions and reinforcement layout

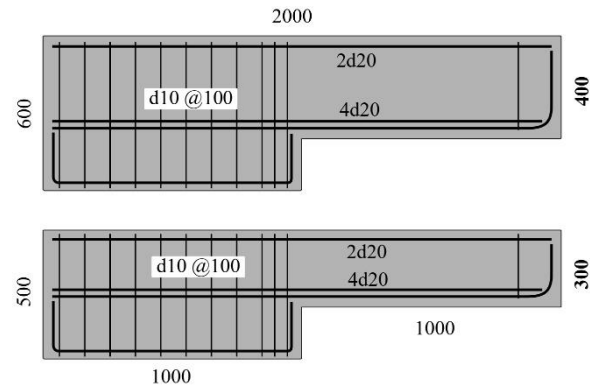


Table 1

Description of beam samples

Series name	Material label	Number of specimens	Depth, mm	Fibre dosage, kg/m ³	Fibre length, mm	Fibre diameter, mm
FRC-3-4-300	FRC-3-4	3	300	40	35	0.5
FRC-3-8-300	FRC-3-8	3	300	80	35	0.5
FRC-5-4-300	FRC-5-4	3	300	40	50	0.75
FRC-5-8-300	FRC-5-8	3	300	80	50	0.75
FRC-3-4-400	FRC-3-4	3	400	40	35	0.5
FRC-3-8-400	FRC-3-8	3	400	80	35	0.5
FRC-5-4-400	FRC-5-4	3	400	40	50	0.75
FRC-5-8-400	FRC-5-8	3	400	80	50	0.75
PC-300	PC300	3	300	NA	NA	NA
PC-400	PC400	3	400	NA	NA	NA

Materials

Five different materials were used in this study. Four of them were different mixes of self-compacting SFRC (SFRSCC). The difference was obtained by using fibres with two different lengths, and two different fibre dosages. There was plain self-compacting concrete (SCC) used for reference. The material labels used in this study (e.g. FRC-3-4 or PC) indicate type of concrete, length of fibres, and fibre dosage. Two labels are used for material: FRC and PC referring to SFRSCC and SCC, respectively. The first number in the material label (3 or 5) refers to the length of the fibres 35 mm or 50 mm, respectively. The last number (4 or 8) refers to the fibre dosage 40 or 80 kg m⁻³, respectively. The dispersion of fibres was evenly distributed along the cross section of the specimens,

with no segregation identified, as it is a self-compacting concrete, see Figure 7.

The SSC mix was made of 280 kg m⁻³ of cement (42.5R), sand (0–4 mm) 727 kg m⁻³, gravel (2–8 mm) 885 kg m⁻³, limestone flour 84 kg m⁻³, fly ash 98 kg m⁻³ and a chemical additive 1.2% of the mass of cement. The water cement ratio was 0.65. The slump-flow class used in this study was SF2 according to the standard EN 206 (European Committee for Standardization, 2021). Material properties of SFRSCC used in the beams were obtained by laboratory tests. For each material, four cubes (edge size of 150 mm) were used to obtain compressive strength according to the standard EN 12390 (European Committee for Standardization, 2019). The mean value of the concrete strength varies from 67.03 MPa to 85.35 MPa

with the coefficient of variation (CoV) 1.0 to 3.0%. The cubes were tested at concrete age of 75 days. Post-cracking flexural tensile strength was determined by notched prisms (150×150×600 mm) under three-point bending tests according to the standard EN 14651 (European Committee for Standardization, 2007). There were 24 specimens for each material tested. Load versus crack mouth opening displacement (CMOD) diagrams of the prisms are given in Figure 2. The residual strength values f_{R1} and f_{R3} at CMOD 0.5 mm and 2.5 mm were in range 5.57–10.34 MPa and 4.77–9.87 MPa, respectively, with CoV 13.2–18.3%. Detailed description of the materials is given in Table 2. The prisms were tested at concrete age of 120 to 132 days.

All the test specimens were manufactured in a concrete plant in middle of January 2022. After casting, they were covered with plastic sheet. All the cubes and prisms were wrapped in plastic film, see Figure 3. The specimens were brought to the laboratory in the end of January and stored in the room conditions till testing. The beam specimens were watered and covered with a plastic sheet, see Figure 4. The tests of the beams were performed during the period from 500 to 900 days.

After the test of the beam specimens, cores were taken from the uncracked and unreinforced regions of the test beams. Actual concrete compressive strength of each beam was obtained by three cores. The results of the strength are given in Figure 5.

The strength of the beams obtained from the extracted cores is very similar to the strength obtained from the cubes. The beams with fibre dosage of 40 kg m⁻³ have higher strength (around 82 MPa) if compared to the beams with fibre dosage of 80 kg m⁻³ (around 72 MPa).

The strength of the beams with plain concrete was smaller – around 69 MPa.

Figure 2
Load–CMOD diagrams of notched prisms

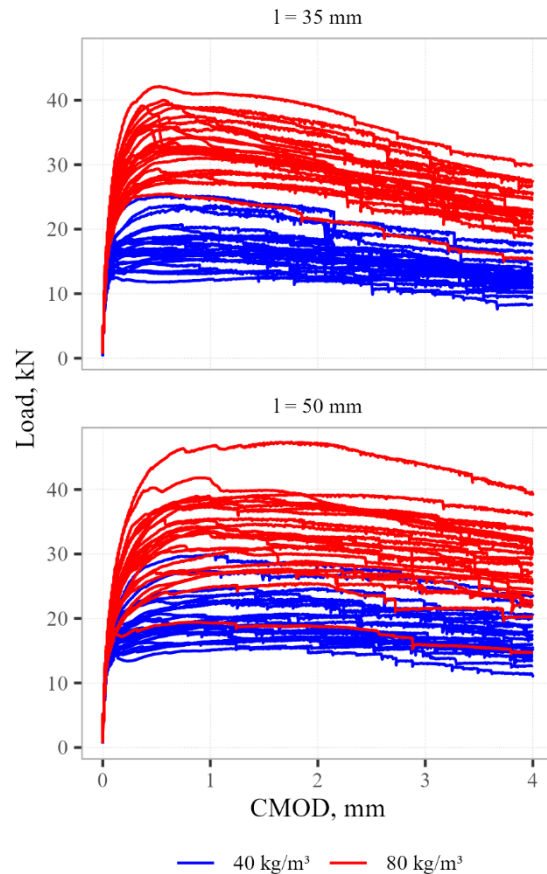


Table 2
Material properties

Material label	f_{cm} , MPa	Coef. of variation (CoV, %)	f_{R1} , MPa	CoV, %	f_{R3} , MPa	CoV, %
FRC-3-4	83.26	2.97	5.57	18	4.77	15.33
FRC-3-8	69.76	2.08	10.34	13.74	8.82	13.23
FRC-5-4	85.35	2.07	6.11	18.23	6.02	17.20
FRC-5-8	77.73	1.55	9.85	18.16	9.87	18.32
PC	67.03	0.99	0	0	0	0

Test setup

The beams were simply supported and set through a three-point bending configuration during the shear test. Form+Test hydraulic test frame Alpha 10-3000 with Zwick Roel load cell with capacity of 600 kN (Class 1) was used. The test setup is shown in Figure. The load was applied at the mid-span by controlling piston displacement at a speed of 0.5 mm/min. The load was transmitted through a spherical steel loading hinge and the beam were supported on rollers at both ends to have free rotation. The test configuration was

aimed to result in shear cracking and eventual shear failure. Mid-span deflection relative to a horizontal steel bar fixed to the beam at the supports was recorded using a Linear Variable Displacement Transducer (LVDT) up to 10 mm as shown in Figure 6(b). In addition, a Digital Image Correlation (DIC) system was utilized to capture vertical displacements and crack evolution. A stochastic black-on-white scattered pattern was added to the surface of the shear span of the beam for the DIC, see Figure 6(a).

Figure 3
Curing of concrete specimens wrapped in plastic film



Figure 4
Beam specimens watered and covered with plastic sheet



Figure 5
Concrete strength determined by cores extracted from test beams after the tests

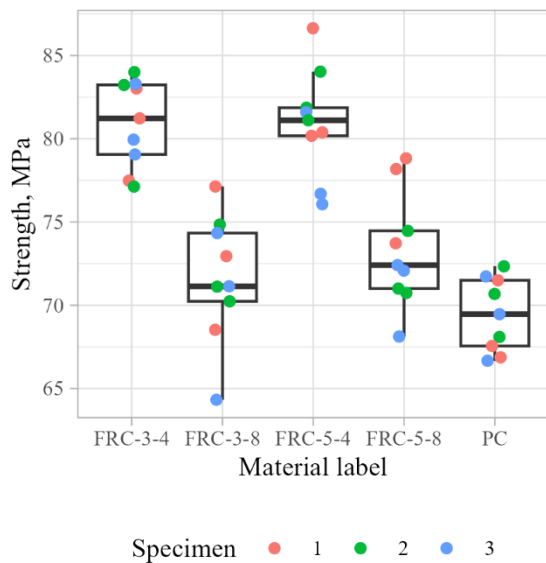
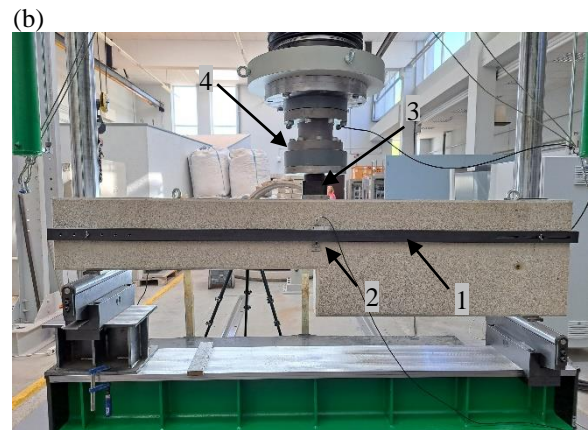
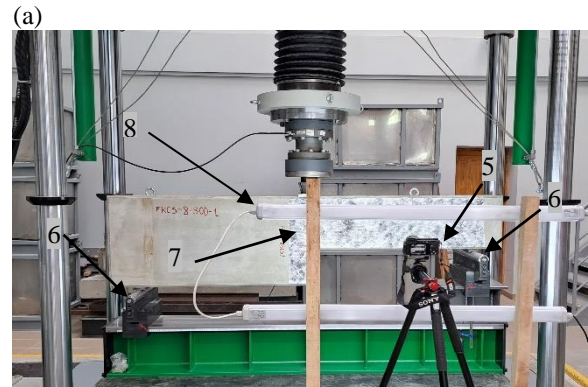


Figure 6
Experimental Test setup: front view (a) and back view (b). (1 – Steel bar, a reference for deflection; 2 – Linear variable differential transformer (LVDT); 3 – Hinge; 4 – Load cell; 5 – Digital camera; 6 – Rollers supports; 7 – painted speckles for Digital image correlation method (DIC); 8 – LED lights)



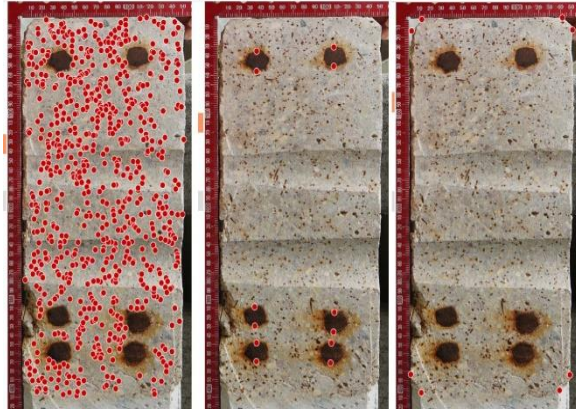
A high-resolution digital mirrorless cameras Sony $\alpha 6400$ equipped with SAMYANG AF 12 mm F/2.0 lenses, was placed at 1 m distance from the specimen. The images were taken with time interval of 5 seconds during the test of each beam. LED lights were used to ensure consistent light intensity during the test. The images were processed using Zeiss Correlate software.

Fibre counting

In order to evaluate the influence of fibres more precisely, a manual fibre counting procedure was applied. The beams were cut at the middle of the span – perpendicular to the beam’s longitudinal axis. The surface was treated with hydrochloric acid to increase the contrast of the fibres. High-resolution images of the cut surfaces together with 90-degree ruler were taken. The geometry of the images was corrected using image manipulation software. Coordinates of every fibre and longitudinal rebars relative to the lower left corner of each section were determined using the WebPlot Digitizer (Rohatgi, 2024) tool as shown in Figure 7.

Figure 7

Fibre counting procedure using WebPlot Digitizer (the red dots show positions of the measured points on the cross-section: fibres, rebars and edges of the cross-section)



Results and Discussion

All of the tested beams failed due to shear in the part with the smaller depth of the beam. The typical failure mode characterised by a group of inclined cracks captured by DIC is given in Figure 8.

The effect of fibre dosage, length of the fibres, and the depth of the beam is evaluated in the load versus deflection diagrams plotted in the Figure 9. The mean values of the maximum load together with the efficiency if compared to the beams made of plain concrete are given in Table 3.

Table 3

Experimentally obtained mean values of maximum load of the beam series

Series name	$F_{max.mean}$ kN	CoV	Efficiency
FRC-3-4-300	248.64	15.7%	177%
FRC-3-8-300	404.92	7.3%	288%
FRC-5-4-300	228.71	3.0%	163%
FRC-5-8-300	329.90	4.1%	234%
PC-300	140.68	12.3%	100%
FRC-3-4-400	312.81	20.6%	166%
FRC-3-8-400	431.44	8.9%	229%
FRC-5-4-400	353.17	10.9%	188%
FRC-5-8-400	533.88	12.0%	283%
PC-400	188.33	27.7%	100%

The efficiency is calculated by dividing the maximum load of a beam with the maximum load of the beam without fibres and of the same height. According to these results, the efficiency of the fibres is in range

163–188% when the dosage was 40 kg m^{-3} and 229–288% when the dosage was 80 kg m^{-3} . Figure 9 shows that fibre amount has higher influence on the stiffness of the beams if compared to concrete compressive strength – the beams with higher fibre dosage (80 kg m^{-3}) had lower compressive strength, see Figure 5, but the stiffness of these beams is higher.

Figure 8

Typical failure mode of the beam specimens captured by DIC

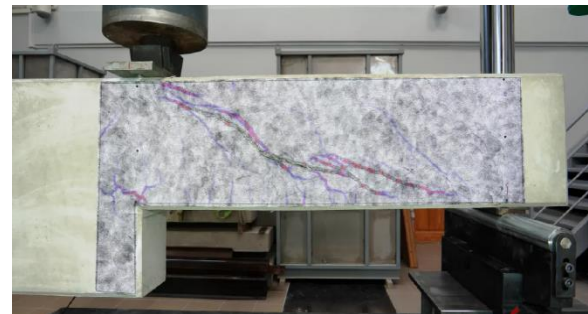
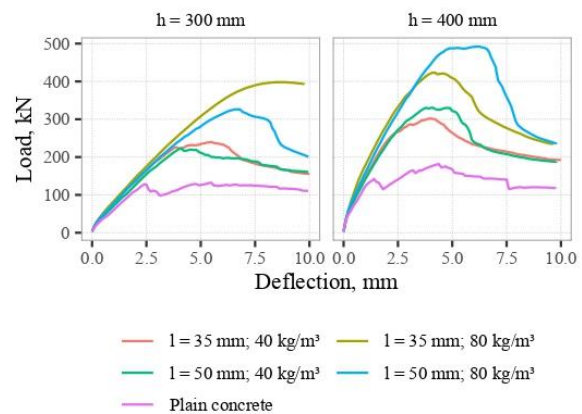


Figure 9

Average load versus deflection diagrams

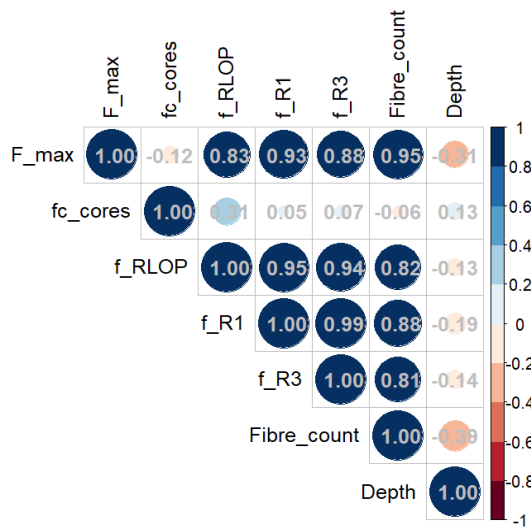


However, beams with 50 mm long fibres exhibited higher abrupt breakdowns due to fibre rupture. This type of rupture was not observed for beams with fibre length of 35 mm. It should be noted that the tests with the notched prisms did not show any similar rupture of the fibres, see Figure 2. That means that SFRC in structures can behave differently than in the prisms tested according to the standard EN 14651 (European Committee for Standardization, 2001). It can be justified by the reduced amount of fibres aligned with the direction of the tensile stresses in the beams' failure zone. If the fibre length exceeds a critical length, the force to pull them out of the concrete matrix is higher than it is necessary to reach the tensile strength of the fibres, leading to an abrupt failure of the beam. In the prisms, where the fibres have a tendency to align with tensile stresses, the abrupt failure is not visible. It complies with the findings by Skadins & Červenka (2024) that the residual tensile properties (tensile

function) should be reduced to have correct predictions of the shear behaviour of SFRC beams without shear links. The experimental study reveals that the length of the fibres can play a significant role. In case of long fibres, the tensile diagram should be reduced to take account for an abrupt failure in shear.

The influence of the different parameters considered in this study is analysed by means of correlation coefficient. Matrices of the coefficients between the parameters like maximum load, concrete compressive strength obtained from the cores, residual flexural tensile strength at different CMOD values, fibre count, and depth is given in Figures 10 and Figure 11 for beams with height of 300 mm and 400 mm, respectively. The study concludes that fibre dosage and residual flexural strengths at various CMOD values (f_{R1} , f_{R3} , f_{RLOP}) are the most crucial parameters in enhancing the beam maximum load capacity (F_{max}). However, the compressive strength obtained from the extracted cores has very small impact on the shear capacity (F_{max}).

Figure 10
Matrix of correlation coefficient between the considered parameters in case of the beams with height of 300 mm



Obviously, there is an influence of the depth of the beam on the shear capacity if beams with height of 300 mm are compared to the same type of beams with height of 400 mm. However, in this case it is small if compared to the effect of fibres. In the Figures 10 and 11, the depth parameter is measured from images as the average depth of the two layers of tensile rebars

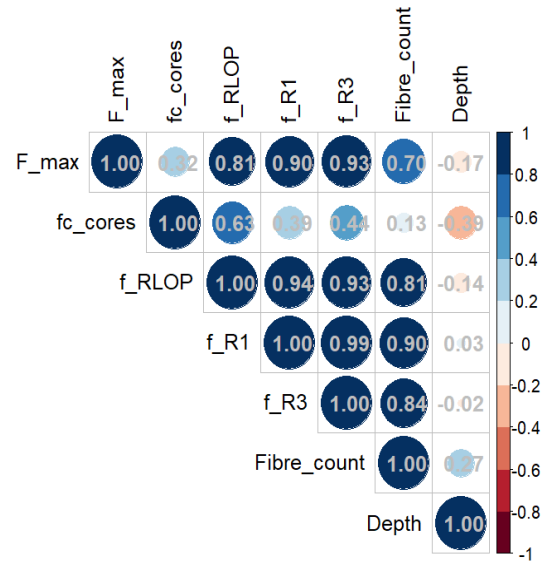
References

Barros, J., Sanz, B., Kabele, P., Yu, R. C., Meschke, G., Planas, J., & Valente, T. (2020). Blind competition on the numerical simulation of steel-fiber reinforced concrete beams failing in shear. *Structural Concrete*, 22(2), 939–67. <https://doi.org/10.1002/suco.202000345>

Batson, G., Jenkins, E., & Spatney, R. (1972). Steel fibers as shear reinforcement in beams. *ACI Journal Proceedings*, 69(10), 640–4. <https://doi.org/10.14359/7151>

using WebPlot Digitizer. As it can be seen from the figures, the actual position of the rebars has no significant influence on the load bearing capacity of the beams.

Figure 11
Matrix of correlation coefficient between the considered parameters in case of the beams with height of 400 mm



Conclusions

An extensive experimental study of self-compacting steel fibre reinforced concrete (SFRSSC) beams with conventional longitudinal reinforcement and without shear reinforcement is carried out. The influence of several factors on the shear capacity is analysed. The following main conclusions can be drawn:

1. Shear capacity of the tested beams are strongly related to the presence of fibres and the corresponding residual tensile strength of SFRSSC.
2. If compared to the beams made of plain concrete, the efficiency of SFRSSC on the shear capacity is in range 163–188% with fibre dosage of 40 kg m⁻³ and 229–288% with fibre dosage of 80 kg m⁻³.
3. Fibre amount has higher influence on the stiffness of the beams if compared to concrete compressive strength.
4. The experimental study reveals that the length of the fibres can play a significant role. The failure of the beams with longer fibres (50 mm) are characterised as abrupt due to the rupture of the fibres. This was not the case for the beams with fibres of length 35 mm.

- Červenka, V. & Gerstle, K. H. (1971) *Inelastic analysis of reinforced concrete panels*. 31, 32–45. <https://cir.nii.ac.jp/crid/1573668924740226560>
- Cohen, M. & Aoude, H. (2012). Shear behavior of SFRC and SCFRC beams. *Proceedings, Annual Conference - Canadian Society for Civil Engineering*, 3, 2557-2566. https://www.researchgate.net/publication/286720231_Shear_behavior_of_SFRC_and_SCFRC_beams
- European Committee for Standardization. (2007). *Test method for metallic fibre concrete—measuring the flexural tensile strength (limit of proportionality (LOP), residual)*. (European Standard: EN 14651:2005+A1:2007). <https://www.lvs.lv/en/products/23255>
- European Committee for Standardization. (2019). *Testing hardened concrete – Part 3: Compressive strength of test specimens* (European Standard: LVS EN 12390-3:2019). <https://www.lvs.lv/lv/products/144353>
- European Committee for Standardization. (2021). *Concrete - Specification, performance, production and conformity* (European Standard: LVS EN 206+A2:2021). <https://www.lvs.lv/lv/products/151971>
- European Committee for Standardization. (2023). *Design of concrete structures – Part 1-1: General rules and rules for buildings, bridges and civil engineering structures* (European Standard: LVS EN 1992-1-1:2023). <https://www.lvs.lv/en/products/162204>
- Fédération internationale du béton. (2013). *fib Model Code of concrete structures 2010*. <https://doi.org/10.1002/9783433604090>
- Kim, K. S., Lee, D. H., Hwang, H. J., & Kuchma, D. A. (2012). Shear behavior model for steel fiber-reinforced concrete members without transverse reinforcements. *Compos B Eng*, 43(5), 2324–2334. <https://doi.org/10.1016/j.compositesb.2011.11.064>
- Kwak, Y. K., Eberhard, M. O., Kim, W. S., & Kim, J. (2002). Shear strength of steel fiber-reinforced concrete beams without stirrups. *ACI Structural Journal*, 99(4), 530–8. <https://doi.org/10.14359/12122>
- Lee, S. C., Cho, J. Y., & Vecchio, F. J. (2016) Analysis of steel fiber-reinforced concrete elements subjected to shear. *ACI Structural Journal*, 113(2), 275–285. <https://doi.org/10.14359/51688474>
- Minelli, F. & Plizzari, G. A. (2010) Shear strength of FRC members with little or no shear reinforcement: a new analytical model. In: Sigrist, V., Foster, S., Minelli, F. & Plizzari, G. (Eds.). *fib Bulletin no 57: shear and punching shear in RC and FRC elements (workshop proceedings)*. Lausanne, Switzerland, FIB (International Federation for Structural Concrete). <http://dx.doi.org/10.35789/fib.BULL.0057.Ch13>
- Narayanan, R. & Darwish, I. Y. S. (1987). Use of steel fibers as shear reinforcement. *ACI Structural Journal*, 84(3), 216–27. <https://doi.org/10.14359/2654>
- Rashid, Y. R. (1968) Ultimate strength analysis of pre-stressed concrete pressure vessels. *Nuclear Engineering and Design*, 7, 334–44. [https://doi.org/10.1016/0029-5493\(68\)90066-6](https://doi.org/10.1016/0029-5493(68)90066-6)
- Rohatgi, A. (2024). WebPlotDigitizer (Version 4.8) [Web based plot digitizer]. <https://automeris.io/WebPlotDigitizer>
- Sahoo, D. R. & Sharma, A. (2014). Effect of steel fiber content on behavior of concrete beams with and without stirrups. *ACI Structural Journal*, 111(5), 1157–66. <https://doi.org/10.14359/51686821>
- Saouma, V. E. (1981) Ingrassia AR. Fracture mechanics analysis of discrete cracking. *Advanced mechanics of reinforced concrete*, 393–416. [https://doi.org/10.1061/\(ASCE\)0733-9445\(1984\)110:4\(871\)](https://doi.org/10.1061/(ASCE)0733-9445(1984)110:4(871))
- Shahnewaz, M. & Alam, M. S. (2014). Improved shear equations for steel fiber-reinforced concrete deep and slender beams. *ACI Structural Journal*, 111(4), 851–860. <https://doi.org/10.14359/51686736>
- Skadins, U. & Červenka, J. (2024). Lessons learnt from blind competition of shear behavior of fiber-reinforced concrete T-beam. *Structural Concrete*, 25(1), 506–525. <https://doi.org/10.1002/suco.202201187>
- Slater, E., Moni, M. & Alam, M. S. (2012). Predicting the shear strength of steel fiber reinforced concrete beams. *Constr Build Mater*, 26(1), 423–436. <https://doi.org/10.1016/j.conbuildmat.2011.06.042>
- Swamy, R. N. & Bahia, H. M. (1985). The effectiveness of steel fibers as shear reinforcement. *Concrete International*, 7(3), 35–40. <https://www.concrete.org/publications/internationalconcreteabstractsportal.aspx?m=details&id=9605>
- Zhang, Y., Gao, Z., Li, Y., & Zhuang, X. (2020) On the crack opening and energy dissipation in a continuum based disconnected crack model. *Finite Elements in Analysis and Design* 170, Article 103333. <https://doi.org/10.1016/j.finel.2019.103333>